DISRUPTION OF TUMOR NECROSIS FACTOR ALPHA RECEPTOR 1 SIGNALING ACCELERATES NAFLD PROGRESSION IN MICE UPON A HIGH FAT DIET

Flavia Lambertucci[1], Ainelén Arboatti[1], María Guillermina Sedlmeier[1], Omar Motiño[2], María de Luján Alvarez[1], María Paula Ceballos[1], Silvina R. Villar[3], Eduardo Roggero[3], Juan A. Monti[1], Gerardo Pisani[4], Ariel D.Quiroga[1], Paloma Martín-Sanz[2,5], Cristina Ester Carnovale[1], Daniel Eleazar Francés[1*] and María Teresa Ronco[1*].

[1]Instituto de Fisiología Experimental (IFISE-CONICET), Suipacha 570, 2000 Rosario, Argentina.
[2]Instituto de Investigaciones Biomédicas Alberto Sols, CSIC-UAM, Arturo Duperier 4, 28029 Madrid, Spain
[3]Instituto de Inmunología. Facultad de Ciencias Médicas, UNR, Suipacha 531, 2000 Rosario, Argentina.
[4]Cátedra de Morfología. Facultad de Ciencias Bioquímicas y Farmacéuticas. Universidad Nacional de Rosario
[5]Centro de Investigación Biomédica en Red de Enfermedades Hepáticas y Digestivas (CIBERehd), Monforte de Lemos 3-5, 28029 Madrid, Spain.

Address correspondence to María Teresa Ronco, PhD. Instituto de Fisiología Experimental (IFISE-CONICET), Suipacha 570, 2000 Rosario, Argentina; Tel +543414305799; e-mail: ronco@ifise-conicet.gov.ar

*These two authors share senior authorship.

Conflict of interest statement: The authors declare no conflict of interest.

ABSTRACT

Obesity is accompanied by a low-grade inflammation state, characterized by increased of pro-inflammatory cytokines levels as tumor necrosis factor alpha (TNFα) and interleukin-1 beta (IL-1β). In this regard, exists a lack of studies in hepatic tissue about the role of TNFα receptor 1 (TNFR1) in the context of obesity and insulin resistance during the progression of non-alcoholic fatty liver disease (NAFLD). The aim of this work was to evaluate the effects of high caloric feeding (HFD) (40% fat, during 16 weeks) on TNFR1 knock-out (TNFR1KO) and Wild Type (WT) mice on liver inflammation induced-apoptosis, insulin resistance, hepatic lipid accumulation and its progression towards non-alcoholic steatohepatitis (NASH). Mechanisms involved in HFD-derived IL-1β release and impairment of insulin signaling are still unknown, so we determined whether IL-1β affects liver insulin sensitivity and apoptosis through TNFR1-dependent pathways. We showed that knocking-out TNFR1 induces an enhanced IL-1β plasmatic release upon HFD feed. This was correlated to higher hepatic and epididymal white adipose tissue (eWAT) mRNA levels. *In vivo* and *in vitro* assays confirmed an impairment in hepatic insulin signaling, in part due to IL-1β-induced decrease of AKT activation and diminution of IRS1 levels, followed by an increase in inflammation, macrophage (resident and recruited) accumulation, hepatocyte apoptotic process and finally hepatic damage. Additionally, TNFR1 KO mice displayed higher levels of pro-fibrogenic markers. TNFR1 signaling disruption upon a HFD leads to an accelerated progression from simple steatosis towards a more severe phenotype with many NASH features, pointing out a key role of TNFR1 in NAFLD progression.

Keywords: High Fat Diet; TNFR1; non alcoholic liver disease; Il-1Beta; insulin resistance; inflammation, IRS1, p-AKT

1. INTRODUCTION

Obesity results from progressive loss of the homeostatic control of food intake and energy expenditure [1]. Obese individuals develop resistance to the cellular actions of insulin, characterized by an impaired ability of insulin to inhibit glucose output from the liver and to promote glucose uptake in fat and muscle. Obesity and insulin resistance are accompanied by a low-grade inflammation state, characterized by increased of pro-inflammatory cytokines in the circulation and tissues. Chronic tissue inflammation has been identified as a major contributor to the decreased insulin sensitivity in obesity [2]. The origin of this inflammation could be related to adipose tissue expansion because the expression of pro-inflammatory cytokines including TNFα and IL-1β are increased in this tissue in the obese state. In this regard, increased macrophage population in adipose tissue is thought to be responsible for this elevated production of cytokines [3,4].

The pro-inflammatory cytokine TNFα plays a key role in a wide variety of physiological processes, including inflammation, proliferation and programmed cell death. TNF receptor 1 (TNFR1) and TNF receptor 2 (TNFR2) are the two main transducers of the TNFα signals in most cells and tissues [5]. Transducing TNFα signals through either receptor results in the activation of inflammatory genes transcription by Nuclear Factor kappa B (NFκB) and Activator Protein 1 (AP-1) [6]. In addition, pro-apoptotic stimulus can be induced by the binding of TNFα to TNFR1 [5,6], that leads to caspase-8 activation, resulting in cleavage of caspase-3 triggering apoptotic cell death.

The role of TNFα in the context of obesity and insulin resistance has been thoroughly explored for many years. However, the participation of each TNFα receptor in obesity-induced insulin resistance had been less studied, existing still controversy on the importance of this inflammatory pathway in the setting of insulin resistance and

obesity-related diseases. While several ‘‘loss-of-function’’ studies reported a partial protection against the development of insulin resistance in mice lacking TNFα [7,8]; other studies suggested that TNFR1 has no role [9] or even a protective one [10] against the development of insulin-resistance. Although blocking TNFα improved insulin resistance in rodents, neutralizing antibodies against TNFα did not significantly improve insulin sensitivity in obese type 2 diabetic patients [11]. On the other hand, it was reported that TNFR1 “gain of function” mutation aggravates nonalcoholic fatty liver disease hallmarks [12]. Even more, and specifically in models of metabolic disorders, it was reported that when are knocking out the two receptors separately, only the absence of TNFR1 showed to be relevant in energetic homeostasis [8].

Non-alcoholic fatty liver disease (NAFLD) is a condition in which excess fat accumulates in the liver of a patient without a history of alcohol abuse and it has become the most common form of liver disease in developed countries. It covers a wide spectrum of hepatic damage in which steatosis with inflammation progresses to non-alcoholic steatohepatitis (NASH), fibrosis and cirrhosis, and hepatocellular carcinoma. Although, NAFLD is closely associated with obesity, insulin resistance and metabolic syndrome, the pathogenesis of NAFLD has not been fully elucidated [13,14].–Assuming the discrepancy of published results and the lack of studies in hepatic tissues about the role of TNFR1 in the context of obesity and insulin resistance in the progression of non-alcoholic fatty liver disease, we first decided to evaluate the effects of high caloric feeding (HFD) on TNFR1 knock-out mice and its association with liver inflammation induced-apoptosis, insulin resistance, steatosis and its progression towards NASH.

Whereas the implication of TNFα in insulin resistance is well documented, little is known about the role of IL-1β. Recent studies demonstrate that expression of IL-1β is

increased in adipose tissue of both obese rodents and humans [15]. Since the mechanisms involved in the induction of IL-1β release by a HFD are still unknown, as well as the associated alteration of insulin signaling and apoptosis, we then determined whether IL-1β affects insulin sensitivity and liver apoptosis through TNFR1-dependent pathways. Here, we showed that knocking out TNFR1 induces IL-1β release which enhances liver insulin resistance followed by an increase in liver inflammation and the progression from simple steatosis towards a phenotype with NASH features.

2. RESEARCH DESIGN AND METHODS

2.1. Experimental Model and Feeding Protocols

Knockout C57BL/6-Tnfrsf1atm1Imx/J (TNFR1 KO) mice (20-25 g body weight; 6-8 weeks) originally obtained from The Jackson Laboratory and gently provided by Dr. Silvia Di Genaro were used in this study along with corresponding age-matched wild-type (WT) mice. Male C57BL/6 mice (WT), 6–8 weeks of age, were provided by the School of Medicine, National University of Rosario. Mice were maintained at the animal facilities of the School of Biochemistry of National University of Rosario. The animals were maintained in light/ dark (12 h light/12 h dark), temperature (22 °C) and humidity-controlled rooms with free access to drinking water. Animals received human care according to criteria outlined in the "Guide for the Care and Use of Laboratory Animals" (National Research Council, Washington D.C.: National Academy Press, 1996). All the experimental protocols were performed according to the Regulation for the Care and Use of Laboratory Animals (Expedient 6109/012 E.C. Resolution 267/02) and approved by the Institutional Animal Use Committee of the National University of Rosario, Argentina.

WT and TNFR1 KO mice were fed with regular chow diet (CHOW)(GEPSA, http://www.gepsa.com) or a 40% high-fat diet (HFD) (Composition in Supplementary table 1) *ad libitum* for 16 weeks. During HFD treatment, body weight and food were recorded every ten days .Upon 16 weeks of treatment, animals were euthanized; blood was obtained by cardiac puncture [16], and plasma prepared for biochemical parameters determination. Liver tissues and eWAT, were snap-frozen in liquid nitrogen and stored at -80°C. Glucose, triglycerides, cholesterol and transaminases AST and ALT were assayed spectrophotometrically in plasma with specific kits from Wiener Lab (Wiener Lab, Rosario, Argentina). Samples of liver tissue were fixed in 4% buffered formalin for

paraffin preparation and then were used for histopathology assessment [17]. For *in vivo* insulin signaling studies, another set of O/N fasted animals were i.p. injected with 0.75 units/kg b.w. of human recombinant insulin and euthanized 15 min later [18].

2.2 Data analysis

Data are expressed as means ± s.e.m. Statistical significance was determined by Student's t-test or the one-way analysis of variance followed by Tukey's test. Analysis was performed by using the statistical software GraphPad Prism 5. A $p<0.05$ was considered statistically significant.

3. RESULTS

3.1 TNFR1 disruption promotes fat liver accumulation

First, in order to assess the diet-induced obesity model, weight gain curve was performed periodically determining the weight of the animals for 16 weeks (Figure 1A). As it was previously described, HFD-WT show an increase in body mass compared to CHOW-WT. However, KO mice showed a significantly lower gain body weight when submitted to high fat diet feeding. This protection from diet induced-obesity found in TNFR1 KO mice was independent of food intake, being the relative food intake of TNFR1 KO not different of WT food intake on either diet (Figure 1B). Table 1 shows plasma biochemical assays. Measurement of plasma glucose, cholesterol and triglycerides levels demonstrated that HFD-KO mice showed lower levels of these parameters when compared to HFD-WT mice. In order to analyze the effect of TNFR1 KO phenotype on peripheral response to insulin we performed the GTT and ITT tests. Glucose tolerance was modified in TNFR1-KO mice showing higher glucose plasma levels than WT mice (Figure 1C). In contrast, intraperitoneal injection of insulin caused a more rapid and pronounced reduction in blood glucose levels in wild type control mice when compared to the HFD-fed mice, observing a similar pattern in KO mice when comparing CHOW and HFD-fed animals (Figure 1C). In these sense, KO mice did not increase insulin plasmatic levels during HF feeding (Table 1). In contrast, HFD fed resulted in a mild elevation of plasma ALT and AST in KO phenotype mice compared with their wild type counter mates (Figure 1D).

It is known that chronic HF feeding causes accumulation of lipids in the liver, leading to fatty liver disease [19]. To determine whether TNFR1 was implicated in this process, hepatic lipids were evaluated. Disruption of TNFR1 signaling induced a marked

steatotic phenotype in HFD-KO mice, with accumulation of fat vacuoles (Figure 1E). In line with this, HFD-KO mice exhibited increased triglyceride content in the liver when compared to HFD-WT (Figure 1F).

3.2 Disruption of TNFR1 signaling increases macrophage liver infiltration

In the progression of nonalcoholic liver disease, steatosis and elevated serum ALT levels are followed by inflammation. [20] Hepatic recruitment of macrophages promotes nonalcoholic steatohepatitis through CCR2 (C-C chemokine receptor type 2) increased expression [21]. Here, we focused our study specifically on the effect that diet has on TNFR1 knock-out phenotype. We observed higher content of hepatic inflammatory infiltrate in HFD-KO mice respect to HFD-WT mice, when were evaluated by histological analysis (Figure 2A). Next, we isolated hepatic non-parenchymal cells (NPCs) from HF-fed mouse livers in order to define the characteristics of innate immune cells, followed by FACS analysis. As illustrated in Figure 2B, livers from TNFR1-KO mice showed an increase in $CD45^{+}F4/80^{+}$ cells suggesting an augmented liver accumulation of macrophages in mice lacking TNFR1. To further assess the different macrophage populations we analyzed $F4/80^{+}$ population cells. We observed an increment in $CD45^{+}F4/80^{high}$ population, which correlates with increased levels of resident hepatic macrophages in HFD KO mice when compared to WT HFD-fed mice (Figure 2C). The same behavior was observed in recruited hepatic macrophages ($CD45^{+}F4/80^{low}$ population) levels (Figure 2C). In this sense, macrophages isolated from KO mice showed an increase in a classical pro-inflammatory activation state (M1), determined by an increase in $CD45^{+}F4/80^{+}CD11c^{+}$ cells when compared to HF-fed-WT (Figure 2D). Also, the number of CCR2-expressing cells was higher in TNFR1-KO suggesting not only a

pro-inflammatory profile of the resident macrophages but also a greater recruitment of pro-inflammatory macrophages to the liver (Figure 2E).

3.3 TNFR1-KO mice show a decreased hepatic insulin signaling

Inflammation, hepatic lipid and glucose metabolism are closely related in the pathogenesis of liver disease, linking insulin resistance to the development of hepatic steatosis and the progression to steatohepatitis [22,23]. We analyzed the insulin activation pathways in the liver. Ours results showed a decrease in p-AKT protein expression in the liver of HFD-KO mice when compared to HFD-WT mice (Figure 3A). The analysis of insulin receptor phosphorylation (p-IR) showed a similar behavior to that observed for p-AKT (Figure 3B). Low insulin receptor substrate 1 (IRS1) mRNA expression and protein levels have been linked to the development of insulin resistance associated to inflammation [24,25]. In this regards, IRS1 protein expression tend to decrease in HF-fed-KO compared to HF-fed-WT mice being in agreement with the activation patterns of p-AKT and p-IR (Figure 3C). In addition, we measured mRNA levels of *Irs1* in liver and eWAT observing lower levels in livers of HFD-KO group comparing to HFD-WT. mRNA levels of *Irs1* in eWAT did not show differences (Figure 3C). Taken together, these data demonstrate that, despite no change in systemic sensitivity to insulin, HF-fed-KO mice have an impaired hepatic insulin action. Given the close relation between inflammation and ERK as one mediator in insulin resistance we measured its phosphorylated levels, observing an increase in its expression in HFD-KO mice compared to HFD-WT (Figure 3D). In addition, to corroborate *in vivo* findings, we performed *in vitro* studies in isolated hepatocytes from mice of all experimental groups. Ours results

demonstrated that on a HFD condition, lower expressions of p-AKT was observed in TNFR1KO mice (Figure 3E).

3.4 TNFR1 deficiency promotes liver apoptosis

It is well established the role of TNFR1 in the development of apoptosis in different tissues. Insulin resistance increased hepatocyte apoptosis is now considered as an important factor contributing to liver disease progression [24]. In this connection, we analyzed if apoptosis process was modified in HF-fed mice lacking TNFR1. As shown in Figure 4, apoptotic index (AI) and caspase-3 activity were increased in HFD-WT when compared to chow fed mice. Analyzing the apoptotic process in mice lacking TNFR1 we found that HF-fed mice exhibited a significantly increase of Apoptotic index and caspase-3 activity (Figure 4A and 4B). This increase observed in HFD-KO was confirmed by TUNEL assay (Figure 4C). Consistently, we observed an increase in the BAX/BCL-x_L ratio in HFD-KO mice (Figure 4D). In this regard, insulin resistance was associated to an augmented hepatic apoptotic state [24]. To support this fact in our model, we determined the levels of BAD protein in hepatic mitochondrial fractions. The pro-apoptotic BAD protein, a member of the BCL-2 family that is involved in the regulation of apoptosis, is inactivated by a mechanism dependent of AKT phosphorylation. Increase of p-AKT levels produce greater BAD phosphorylation (and lower BAD translocation into the mitochondria), promoting cell survival instead of apoptosis. On HF diet condition, a significant increase in BAD localization in mitochondrial fraction was observed when compared to levels observed on CHOW diet condition. In addition, KO mice fed with HFD exhibited a greater mitochondrial localization of BAD, which could be associated to lower AKT activation, and so promoting apoptotic cell death (Figure 4E). To corroborate these results, and using flow cytometry analysis, we observed an increase in

hipoploide (a hallmark of apoptotic cells) percentage of cells in HFD-KO mice when compared to HFD-WT mice (Figure 4F).

3.5 TNFR1-KO mice exhibit features of a pro-inflammatory state

Given the increase of macrophage liver infiltration in KO HF-fed mice, we decided to examine the expression of several inflammation makers. Plasma cytokine levels demonstrated that HF feeding induced the release of IL-1β. In this regard, we found that TNFR1-KO mice showed significantly higher levels of IL-1β when compared to WT mice (Figure 5A). In this sense, HF-fed-KO mice showed a 7-fold increase in IL-1β plasma levels when compared to HF-fed-WT mice, a more discrete increase in IL-6, while TNFα plasma levels remain unchanged between HF-fed animals. In order to identify a possible source of IL-1β we determined hepatic and eWAT mRNA expression of pro-inflammatory cytokines in HF-fed mice. We found that HF-fed-KO mice showed an increased expression of *Il1β*, *Il6* and *Tnfα* both in liver and eWAT when compared to HF-fed-WT mice (Figure 5B and 5C). Furthermore, the expression of IL-1β receptor was increased in plasmatic membrane of liver from mice lacking TNFR1 fed the HFD, suggesting that the liver could be acting both as the source and target tissue for IL-β1 (Figure 5D). Macrophages express high levels of the innate immune Toll-like receptor 4 (TLR 4), and this receptor has been implicated as an important player in chronic low-grade inflammation associated to obesity [26]. We found that TLR4 protein expression was increased in HFD-KO mice when compared to HFD-WT mice in plasmatic

membrane of total livers. According with our data, activation of TLR4 signaling leads to the generation of pro-inflammatory cytokines as IL-1β (Figure 5E).

3.6 Apoptosis and insulin resistance in HFD-KO mice are IL-1β-dependent

In order to investigate whether IL-1β is involved in the development of insulin resistance in HF-fed-KO mice, we performed *in vitro* studies in isolated hepatocytes from WT and TNFR1 KO mice. Hepatocytes were pretreated with 10 or 50 ng/ml of IL-1β for 24 hours, and in the case of insulin signaling studies, followed by 10 nM or 50 nM insulin for 7 min. As shown in figure 6A, despite KO hepatocytes were constitutively insulin resistant, IL-1β is able to inhibit hepatocyte AKT phosphorylation in response to insulin (50 nM). In addition, we analyzed the expression of IRS1 and we observed that IL-1β treatment reduced total IRS1 levels in WT and KO isolated hepatocytes, although this reduction is more significant in the KO genotype (Figure 6B). In these conditions, AKT protein activation is diminished in hepatocytes from KO mice probably due to the ability of IL-1β to diminish IRS1 protein levels. Then, we analyzed the effect of IL-1β treatment in the induction of caspase-3 activity as a measured of cell death. After IL-1β stimulus, we observed an increase in caspase-3 activity only in hepatocytes isolated from KO mice (Figure 6C). These results could explain the modifications observed in the *in vivo* studies of the apoptotic and insulin signaling pathways, suggesting a more sensitive response in KO liver mice to IL-1β action.

3.7 TNFR1 disruption drives the progression from simple steatosis to a more severe stage of NAFLD in a HFD

To investigate if the augmented inflammation, insulin resistance and hepatocyte apoptosis observed in KO-HF-fed mice was accompanied by increased hepatic fibrosis,

a predominant feature of advanced NASH, we assessed the liver architecture for the evaluation of hepatic collagen deposition in HF-fed mice. Whereas fibrosis was absent in HF-fed-WT mice, we observed mild fibrosis by Sirius Red and Masson's Trichrome staining of liver sections in HF-fed-KO mice (Figure 7A). Figure 7B shows the fibrosis score in HF-fed mice assessed through histological analysis, while Figure 7C represents collagen content in these HF-fed groups measured by Sirius Red staining. In figures 7B and C we observed the same increase in these parameters in KO mice with respect to WT fed with high fat diet.Ours results showed that KO phenotype under HFD exhibited inflammation and bile duct proliferation mainly in portal zone. These results indicate that disruption of TNFR1 signaling promotes liver damage and the progression from simple steatosis towards a more severe liver disease phenotype in mice feeding with HFD.

4. DISCUSSION

Obesity, insulin resistance and its associated complications are increasing dramatically and have become an important global health issue. The incomplete understanding of the pathological mechanism of these diseases is the reason why the therapeutic strategies remain unsatisfactory.

Little is known about the role of TNFR1 signaling in the development of obesity, insulin resistance and liver damage. Here, we aimed to gain more knowledge about the biological significance of TNFR1 deletion in the development of insulin resistance and in the progression of steatohepatitis using a "loss of function" murine model. In this study we found that disruption of TNFR1 signaling increases plasma IL-1β levels, exacerbates liver obesity-related inflammatory response, insulin resistance, and liver damage in mice fed with a HFD.

Chronic HFD treatment causes accumulation of lipids in the liver, a process leading to fatty liver disease [19]. Under these nutritional conditions, HFD-KO mice developed more severe steatosis, including higher accumulation of lipid vacuoles and a significant increase in liver triglycerides (TG) content than HFD-WT. In addition, ALT and AST activities significantly correlated with liver injury. It was previously reported in mutant mice expressing non-sheddable TNFR1s ($p55^{\Delta ns/\Delta ns}$), which exhibit persistent expression of the receptor at the cell surface, that TNFR1 constitutive signaling is not associated to the development of hepatic steatosis. Even more, advanced NASH-like phenotypes were observed in the livers of these mutant mice fed a HFD compared to wild type mice, suggesting a possible role of TNFR1 during the progression of NAFLD pathogenesis [12]. In the other hand, and confirming the key role of TNFR1 in NAFLD progression and NASH pathogenesis, we observed that the deletion of TNFR1 in obese

mice leads to an exacerbation of liver steatosis and inflammation suggesting a cross-talk between the TNFR1 and liver lipid accumulation as an important mediator in the pathophysiology of NASH.

Hepatic resident macrophages or Kupffer cells (KC) are central players in the development of NAFLD, by secreting pro-inflammatory cytokines, recruiting other inflammatory immune cells and so promoting hepatic inflammation and insulin resistance. In the present work, we found that the lack of TNFR1 enhanced liver inflammation. To define the characteristics of innate immune cells, we isolated NPCs from obese mice and found that livers from TNFR1-KO mice showed an increase in $CD45^{+}F480^{+}$ cells under fat fed condition, suggesting macrophage hepatic accumulation in this genotype. Despite the KCs classical activation pathways, it can be directly activated by cytokines, adipokines or free fatty acids secreted from adipose tissue which induce the polarization of KCs to the pro-inflammatory M1 phenotype. In this regard, the analysis of $CD45^{+}/F480^{+}$ population revealed an increase in the number of $CD45^{+}F4/80^{+}CD11c^{+}$ cells in mice lacking TNFR1 fed with high fat diet, a feature associated with NASH progression [27] and with a pro-inflammatory M1 state [20]. The exacerbated release of M1 Kupffer-cell-derived mediators contributes to the pathogenesis of liver steatosis, the recruitment of inflammatory immune cells, and the activation of fibrotic process [28]. In line with this, ours results demonstrated, for the first time, that TNFR1 disruption not only leaded to an impaired inflammatory profile of liver resident macrophage, but also to an increased hepatic macrophage recruitment, suggested by an exacerbated number of CCR2-expressings cells.

Because NAFLD and insulin resistance are associated pathologies, we tested whether the chronic, low-grade inflammation and liver damage observed in HF-fed-KO

mice contributed to the development of insulin resistance. Although those mice showed a diminished weight gain and normal systemic sensitivity to insulin, they were able to develop intrahepatic insulin resistance. In these sense and in accordance with ours results, others authors reported that MCD-fed mice exhibited lost enhanced glucose tolerance and insulin hypersensitivity [29,30]. We hypothesized that, TNFR1-KO mice behaves as MCD-diet mice when are subjected to HFD, probably as a consequence of hepatic steatosis and inflammation that may lead to hepatic resistance, by a direct interference with effectors of intracellular IR-dependent signaling pathways. Other studies provide evidence for the possibility that liver insulin resistance is dependent on autocrine and paracrine actions of IL-1β [31]. Our results demonstrated that plasmatic levels of IL-1β were increased in WT mice fed a HFD. To date, little is known on the pro-inflammatory cytokine profile in mice lacking TNFR1 fed a HFD. We found that, the disruption of TNFR1 induces a 7-fold increase in plasma IL-1β levels in HF-fed-KO mice, indicating that the lack of the receptor somehow is implicated in the deregulation of cytokine production. Moreover, pro-inflammatory mRNA markers were also higher in hepatic tissue from HF-fed-KO mice when compared to WT mice after HFD. In a recent study, it was reported that following LPS exposure, TNFα KO mice produce three times the amount of IL-1β compared to WT mice, suggesting a cross-talk in of this cytokines pathways [32]. The activation of TLR4 signaling leads to the generation of pro-inflammatory cytokines, including IL-1β, through the up-regulation of several transcription factors. Interestingly, we observed an increase in TLR4 expression HFD-KO mice in association with the excess of inflammatory macrophages, the mRNA expression, and the rise of plasmatic levels of IL-1β. According to our results, we suggest that disruption of TNFR1 leads to an increased number of KCs after a HFD which could contribute to amplify the hepatic inflammatory response through the activation of TLR4

signaling. Additionally, all these pro-inflammatory mediators might be able to lead to hepatic toxicity and impairment of liver function.

In classical immune response, IL-1β is more frequently viewed to exert local cell-cell, rather than systemic effects, suggesting that it is more likely involved in paracrine (and/or autocrine) interactions rather than mediating endocrine communication [31]. In this sense, HFD-KO mice showed a higher expression of IL-1β receptor in plasma membrane of hepatocytes, suggesting that IL-1β synthesis may take place in the liver and once released, mature IL-1β is able to bind to hepatocyte receptors. The potential of the liver as a metabolic target for IL-1β in obesity could be inferred from the finding that the IL-1 receptor a (IL-1Ra) antagonist not only improved stimulated insulin levels, but also decreased fasting glucose, largely reflecting attenuated hepatic glucose production [33]. The results obtained in our study demonstrated that the disruption of TNFR1 induces a higher increase of plasmatic IL-1β that is correlated with an augmented expression of its hepatic mRNA levels. Furthermore, when TNFR1-KO animals were feeding with a High Fat Diet there was an exacerbated rise of plasmatic IL-1β concomitantly with an impairment of hepatic insulin signaling. This phenomenon was also examined and observed in isolated hepatocytes. KO hepatocytes were constitutively insulin resistant, probably as a consequence of endogenous IL-1β levels in CHOW-KO mice. Otherwise, taken together, our *in vitro* studies allow us to hypothesize an IL-1β effect over hepatic insulin resistance exacerbated in KO hepatocytes, which is due in part to the impairment of AKT activation and the reduction of IRS1 protein levels.

In line with the notion that insulin exerts anti-apoptotic functions in many cell types, [34], in a previous work we demonstrated that hepatic insulin resistance was associated with the apoptotic process [19]. Here, our results showed that HFD-KO mice

exhibited an increased apoptotic process in the liver. In addition, in a study performed in liver biopsy of patient with NASH, it has been reported a positive correlation between the hepatic mRNA levels of IRS1, IRS2, p85a, and anti-apoptotic mediators, indicating that impairment of the hepatic insulin signaling pathway is closely related to enhanced hepatocyte apoptosis in NASH [24]. A large body of evidence has shown the mediation by AKT in the anti-apoptotic action of insulin in a variety of cell types [35–37]. AKT is required to maintain the pro-apoptotic protein BAD inactive [38]. Phosphorylated BAD is sequestered away from the site of action in the mitochondria [39,40]. In this connection we analyzed mitochondrial BAD localization and we noted that HFD-KO mice showed an increase in BAD expression in the mitochondria, correlating with a diminution of AKT activation. These results demonstrated that the disruption of TNFR1 in mice fed with HFD induces apoptosis in part due to insulin resistance and the translocation of BAD to the mitochondria.

In the other hand, we could not discard a direct effect of IL-1β on the apoptotic process. Sustained inflammation can trigger apoptosis and pyroptosis, another form of programmed cell death defined as a caspase-1-dependent cell death that is associated with the generation IL-1β [41]. We found increased apoptosis both *in vivo* and *in vitro*, which is associated with increased production of IL-1β and caspase-3 activities. Further studies are necessary to determine the implication of inflammosome and pyroptosis in TNFR1 KO mice feed with HFD. Overall, these results suggest that IL-1β induces apoptosis in the livers of TNFR1 KO mice. It is well documented that IL-1β treatment induces a

sustained activation of ERK and p38MAPK, which are known to be implicated in the induction of the apoptotic process [42], facts also observed in our model.

Judging for our results that indicated an important role for TNFR1 in the progression of NAFLD, we investigated the effect of the deletion of TNFR1 on hepatic fibrosis, an advanced hallmark of NASH. We observed increased level of collagen by histologic analysis in HF-fed-KO mice when compared to HF-fed-WT mice. According, a clinical study demonstrated that hepatic insulin signaling is markedly impaired in NASH patients, and downregulation of hepatic insulin mediators is associated with enhanced hepatocyte apoptosis and fibrogenesis [24]. In line with this, we demonstrated that TNFR1 signaling disruption, in a context of HFD feeding, leads to a progression from simple steatosis toward a more serious phenotype with many NASH features, including not only inflammation, insulin resistance but also apoptosis and fibrosis.

4.1 Conclusion

The present study reveals a critical role for TNFR1 in the development of a hepatic metabolic disease. Our findings show for the first time that the disruption of TNFR1 signaling causes systemic insulin resistance due to an increased IL-1β production, which in turn, induces hepatic lipid accretion and activation of the apoptotic machinery, leading

to inflammation and the develop of a more severe form of NAFLD. This evidences point out a novel functional role for TNFR1 in the pathogenesis and progression of NAFLD.

5. Funding and acknowledgment

This work was supported by research grants from Consejo Nacional de Investigaciones Científicas y Técnicas (PIP-CONICET 112201500508, C.E.C) and SAF2016-75004-R and SAF2015-70270-REDT (MINECO, Spain) to P.M.S. and O.M. We especially wish to thank Celeste Molina, Alejandra Martínez and Julián Guercetti for their valuable technical assistance, and to Mara Ojeda for flow cytometry analysis.

6. REFERENCES

[1] Schwartz MW. Central nervous system regulation of food intake. Obesity (Silver Spring) 2006;14 Suppl 1:1S–8S. doi:10.1038/oby.2006.275.

[2] Morinaga H, Mayoral R, Heinrichsdorff J, Osborn O, Franck N, Hah N, et al. Characterization of Distinct Subpopulations of Hepatic Macrophages in HFD/Obese Mice. Diabetes 2015;64:1120–30. doi:10.2337/db14-1238.

[3] Marette A. Molecular mechanisms of inflammation in obesity-linked insulin resistance. Int J Obes Relat Metab Disord 2003;27 Suppl 3:S46-8. doi:10.1038/sj.ijo.0802500.

[4] Wellen KE, Hotamisligil GS. Inflammation, stress, and diabetes. J Clin Invest 2005;115:1111–9. doi:10.1172/JCI25102.

[5] Hehlgans T, Pfeffer K. The intriguing biology of the tumour necrosis factor/tumour necrosis factor receptor superfamily: players, rules and the games. Immunology 2005;115:1–20. doi:10.1111/j.1365-2567.2005.02143.x.

[6] Locksley RM, Killeen N, Lenardo MJ. The TNF and TNF receptor superfamilies: integrating mammalian biology. Cell 2001;104:487–501.

[7] Uysal KT, Wiesbrock SM, Marino MW, Hotamisligil GS. Protection from obesity-induced insulin resistance in mice lacking TNF-alpha function. Nature 1997;389:610–4. doi:10.1038/39335.

[8] Uysal KT, Wiesbrock SM, Hotamisligil GS. Functional analysis of tumor necrosis factor (TNF) receptors in TNF-alpha-mediated insulin resistance in genetic obesity. Endocrinology 1998;139:4832–8.

doi:10.1210/endo.139.12.6337.

[9] Pamir N, McMillen TS, Kaiyala KJ, Schwartz MW, LeBoeuf RC. Receptors for tumor necrosis factor-alpha play a protective role against obesity and alter adipose tissue macrophage status. Endocrinology 2009;150:4124–34. doi:10.1210/en.2009-0137.

[10] Toda K, Hayashi Y, Saibara T. Deletion of tumor necrosis factor-alpha receptor type 1 exacerbates insulin resistance and hepatic steatosis in aromatase knockout mice. Biochim Biophys Acta 2010;1801:655–64. doi:10.1016/j.bbalip.2010.03.002.

[11] Hotamisligil GS, Budavari A, Murray D, Spiegelman BM. Reduced tyrosine kinase activity of the insulin receptor in obesity-diabetes. Central role of tumor necrosis factor-alpha. J Clin Invest 1994;94:1543–9. doi:10.1172/JCI117495.

[12] Aparicio-Vergara M, Hommelberg PPH, Schreurs M, Gruben N, Stienstra R, Shiri-Sverdlov R, et al. Tumor necrosis factor receptor 1 gain-of-function mutation aggravates nonalcoholic fatty liver disease but does not cause insulin resistance in a murine model. Hepatology 2013;57:566–76. doi:10.1002/hep.26046.

[13] Angulo P. Nonalcoholic fatty liver disease. N Engl J Med 2002;346:1221–31. doi:10.1056/NEJMra011775.

[14] Dyson J, Jaques B, Chattopadyhay D, Lochan R, Graham J, Das D, et al. Hepatocellular cancer: the impact of obesity, type 2 diabetes and a multidisciplinary team. J Hepatol 2014;60:110–7. doi:10.1016/j.jhep.2013.08.011.

[15] Martin MU, Wesche H. Summary and comparison of the signaling mechanisms

of the Toll/interleukin-1 receptor family. Biochim Biophys Acta 2002;1592:265–80.

[16] Francés DE a, Ingaramo PI, Mayoral R, Través P, Casado M, Valverde ÁM, et al. Cyclooxygenase-2 over-expression inhibits liver apoptosis induced by hyperglycemia. J Cell Biochem 2013;114:669–80. doi:10.1002/jcb.24409.

[17] Motiño O, Agra N, Brea Contreras R, Domínguez-Moreno M, García-Monzón C, Vargas-Castrillón J, et al. Cyclooxygenase-2 expression in hepatocytes attenuates non-alcoholic steatohepatitis and liver fibrosis in mice. Biochim Biophys Acta 2016;1862:1710–23. doi:10.1016/j.bbadis.2016.06.009.

[18] Francés DE, Motiño O, Agrá N, González-Rodríguez A, Fernández-Álvarez A, Cucarella C, et al. Hepatic cyclooxygenase-2 expression protects against diet-induced steatosis, obesity and insulin resistance. Diabetes 2015;64:1522–31. doi:10.2337/db14-0979.

[19] Francés DE, Motiño O, Agrá N, González-Rodríguez A, Fernández-Álvarez A, Cucarella C, et al. Hepatic cyclooxygenase-2 expression protects against diet-induced steatosis, obesity and insulin resistance. Diabetes 2015;64:1522–31. doi:10.2337/db14-0979.

[20] Lumeng CN, Bodzin JL, Saltiel AR. Obesity induces a phenotypic switch in adipose tissue macrophage polarization. J Clin Invest 2007;117:175–84. doi:10.1172/JCI29881.

[21] Miura K, Yang L, van Rooijen N, Ohnishi H, Seki E. Hepatic recruitment of macrophages promotes nonalcoholic steatohepatitis through CCR2. Am J Physiol Gastrointest Liver Physiol 2012;302:G1310-21. doi:10.1152/ajpgi.00365.2011.

[22] Bechmann LP, Hannivoort RA, Gerken G, Hotamisligil GS, Trauner M, Canbay

A. The interaction of hepatic lipid and glucose metabolism in liver diseases. J Hepatol 2012;56:952–64. doi:10.1016/j.jhep.2011.08.025.

[23] Gaggini M, Morelli M, Buzzigoli E, DeFronzo RA, Bugianesi E, Gastaldelli A. Non-alcoholic fatty liver disease (NAFLD) and its connection with insulin resistance, dyslipidemia, atherosclerosis and coronary heart disease. Nutrients 2013;5:1544–60. doi:10.3390/nu5051544.

[24] García-Monzón C, Lo Iacono O, Mayoral R, González-Rodríguez A, Miquilena-Colina ME, Lozano-Rodríguez T, et al. Hepatic insulin resistance is associated with increased apoptosis and fibrogenesis in nonalcoholic steatohepatitis and chronic hepatitis C. J Hepatol 2011;54:142–52. doi:10.1016/j.jhep.2010.06.021.

[25] Liu Z, Patil IY, Jiang T, Sancheti H, Walsh JP, Stiles BL, et al. High-Fat Diet Induces Hepatic Insulin Resistance and Impairment of Synaptic Plasticity. PLoS One 2015;10:e0128274. doi:10.1371/journal.pone.0128274.

[26] Shi H, Kokoeva M V, Inouye K, Tzameli I, Yin H, Flier JS. TLR4 links innate immunity and fatty acid-induced insulin resistance. J Clin Invest 2006;116:3015–25. doi:10.1172/JCI28898.

[27] Itoh M, Suganami T, Kato H, Kanai S, Shirakawa I, Sakai T, et al. CD11c+ resident macrophages drive hepatocyte death-triggered liver fibrosis in a murine model of nonalcoholic steatohepatitis. JCI Insight 2017;2. doi:10.1172/jci.insight.92902.

[28] Sica A, Invernizzi P, Mantovani A. Macrophage plasticity and polarization in liver homeostasis and pathology. Hepatology 2014;59:2034–42. doi:10.1002/hep.26754.

[29] Leclercq IA, Lebrun VA, Stärkel P, Horsmans YJ. Intrahepatic insulin resistance

in a murine model of steatohepatitis: effect of PPARgamma agonist pioglitazone. Lab Invest 2007;87:56–65. doi:10.1038/labinvest.3700489.

[30] Rinella ME, Elias MS, Smolak RR, Fu T, Borensztajn J, Green RM. Mechanisms of hepatic steatosis in mice fed a lipogenic methionine choline-deficient diet. J Lipid Res 2008;49:1068–76. doi:10.1194/jlr.M800042-JLR200.

[31] Nov O, Kohl A, Lewis EC, Bashan N, Dvir I, Ben-Shlomo S, et al. Interleukin-1β May Mediate Insulin Resistance in Liver-Derived Cells in Response to Adipocyte Inflammation. Endocrinology 2010;151:4247–56. doi:10.1210/en.2010-0340.

[32] De Santis S, Kunde D, Galleggiante V, Liso M, Scandiffio L, Serino G, et al. TNFα deficiency results in increased IL-1β in an early onset of spontaneous murine colitis. Cell Death Dis 2017;8:e2993. doi:10.1038/cddis.2017.397.

[33] Larsen CM, Faulenbach M, Vaag A, Vølund A, Ehses JA, Seifert B, et al. Interleukin-1-receptor antagonist in type 2 diabetes mellitus. N Engl J Med 2007;356:1517–26.

[34] Navarro P, Valverde AM, Benito M, Lorenzo M. Insulin/IGF-I rescues immortalized brown adipocytes from apoptosis down-regulating Bcl-xS expression, in a PI 3-kinase- and map kinase-dependent manner. Exp Cell Res 1998;243:213–21. doi:10.1006/excr.1998.4168.

[35] Lawlor MA, Alessi DR. PKB/Akt: a key mediator of cell proliferation, survival and insulin responses? J Cell Sci 2001;114:2903–10. doi:10.1042/bst0290001.

[36] Xi X, Gao L, Hatala DA, Smith DG, Codispoti MC, Gong B, et al. Chronically elevated glucose-induced apoptosis is mediated by inactivation of Akt in cultured Müller cells. Biochem Biophys Res Commun 2005;326:548–53.

doi:10.1016/j.bbrc.2004.11.064.

[37] Ricci C, Jong CJ, Schaffer SW. Proapoptotic and antiapoptotic effects of hyperglycemia: role of insulin signalingThis article is one of a selection of papers published in the special issue Bridging the Gap: Where Progress in Cardiovascular and Neurophysiologic Research Meet. Can J Physiol Pharmacol 2008;86:166–72. doi:10.1139/Y08-021.

[38] Fernando RI, Wimalasena J. Estradiol abrogates apoptosis in breast cancer cells through inactivation of BAD: Ras-dependent nongenomic pathways requiring signaling through ERK and Akt. Mol Biol Cell 2004;15:3266–84. doi:10.1091/mbc.E03-11-0823.

[39] Datta SR, Dudek H, Tao X, Masters S, Fu H, Gotoh Y, et al. Akt phosphorylation of BAD couples survival signals to the cell-intrinsic death machinery. Cell 1997;91:231–41.

[40] Yano S, Tokumitsu H, Soderling TR. Calcium promotes cell survival through CaM-K kinase activation of the protein-kinase-B pathway. Nature 1998;396:584–7. doi:10.1038/25147.

[41] Lebeaupin C, Proics E, de Bieville CHD, Rousseau D, Bonnafous S, Patouraux S, et al. ER stress induces NLRP3 inflammasome activation and hepatocyte death. Cell Death Dis 2015;6:e1879. doi:10.1038/cddis.2015.248.

[42] Larsen CM, Wadt KA, Juhl LF, Andersen HU, Karlsen AE, Su MS, et al. Interleukin-1beta-induced rat pancreatic islet nitric oxide synthesis requires both the p38 and extracellular signal-regulated kinase 1/2 mitogen-activated protein kinases. J Biol Chem 1998;273:15294–300.

[43] Liang W, Menke AL, Driessen A, Koek GH, Lindeman JH, Stoop R, et al.

Establishment of a general NAFLD scoring system for rodent models and comparison to human liver pathology. PLoS One 2014;9:e115922. doi:10.1371/journal.pone.0115922.

FIGURE LEGENDS

Figure 1. ***Assessment of diet-induced insulin resistance model and fat liver accumulation***.

(A) Body weight was registered periodically for Wild type (WT) (circle) or TNFR1 KO (square) mice fed on standard rodent chow (white) or high-fat diet (black). Initial and final body weight and ***(B)*** energy intake, determined over the experimental period of 16 weeks and expressed as Kcal/day. ***(C)*** Glucose tolerance test (GTT) after 16 h fasting. Graph represents area under the curve (AUC) during GTT, and Insulin Tolerance Test (ITT) after 6 h fasting. Graph represent constant of glucose disappearance (Kitt) obtained from ITT. ***(D)*** Plasma levels of AST and ALT in WT and KO mice fed with HFD. ***(E)*** Representative images of hematoxylin/eosin (H&E) stained liver slices from HFD WT and HFD KO mice (200X). Determination of Steatosis grade according to Liang *et al.* score [43]. ***(F)*** Triglycerides content in total liver homogenate. Data are expressed as means ± s.e.m (n=4–5 per group). *$p<0.05$ *vs* CHOW WT. # $p<0.05$ *vs* HFD WT. †$p<0.05$ *vs* CHOW KO.

Figure 2. ***TNFR1 KO mice exhibit macrophages liver infiltration under HFD.***

(A) Representative images of H&E stained liver sections taken from HFD WT and HFD KO mice (100X), where arrows indicate inflammatory infiltrates, and quantification of inflammation score. ***(B)*** Analysis of $CD45^+F4/80^+$ isolated non-parenchymal liver cells; ***(C)*** $CD45^+F4/80^{high}$ and $CD45^+F4/80^{low}$ populations. ***(D)*** Analysis of $CD11c^+$ population from the $CD45^+F4/80^+$ gated cells in ***(B)***. ***(E)*** $CCR2^+$ population from $F4/80^+CD11b^+$

gated cells. Values are expressed as percentage. Data are expressed as means ± s.e.m (n=4-5 per group). # p<0.05 *vs* HFD WT.

Figure 3. ***TNFR1 disruption attenuated hepatic insulin signaling in mice fed with HFD.***

(A) Immunoblot analysis and densitometry of liver lysate p-AKT/AKT ratio in WT and TNFR1 KO mice livers upon regular chow or high fat diet feeding; ***(B)*** p-IR/IR ratio in liver plasmatic membrane enriched fraction and ***(C)*** IRS1 immunoblot, densitometric analysis in liver lysate and mRNA levels of *Irs1* measured in liver and eWAT by real-time quantitative PCR and normalized to the expression of G*apdh* mRNA. Data are expressed as mean ± s.e.m (n=4-5 per group). *p<0.05 *vs* CHOW WT. # p<0.05 *vs* HFD WT. †p<0.05 *vs* CHOW KO. ***(D)*** p-ERK/ERK ratio in liver lysate. Bar graph shows the mean ± s.e.m (n=4-5 per group). Values are expressed as percentage of control (CHOW WT). *p<0.05 *vs* CHOW WT. #p<0.05 *vs* HFD WT. †p<0.05 *vs* CHOW KO. ***(E)*** Isolated hepatocytes from WT and TNFR1 KO mice fed on standard rodent chow or high-fat diet were incubated in DMEM/F12 medium with supplements. After 4 hours of culture and 2 hours of starving (2% FBS), hepatocytes were stimulated with 0, 10 or 50 nM insulin and p-AKT/AKT ratio was analyzed by Western Blot. Values are expressed as percentage of control (CHOW WT + Insulin 50 nM). *p<0.05 *vs* CHOW WT (insulin 10 nM). †p<0.05 *vs* CHOW WT (insulin 50 nM). #p<0.05 *vs* HFD KO (insulin 50 nM).

Figure 4. ***Apoptotic cell death is increased in TNFR1 KO mice.***

(A) Apoptotic cells were estimated by the apoptotic index (AI) assessed in H&E stained liver slices ***(B)*** Caspase-3 activitiy was evaluated by a fluorometric assay in liver lysates from four experimental groups. Bar graphs represent Relative Fluorescence Units (RFU) ***(C)*** Representative images of apoptotic cells evaluated by TUNEL assay. ***(D)***

Mitochondrial levels of pro-apoptotic BAX and anti-apoptotic BCL-x_L proteins were analyzed by Western blot. BAX:BCL-x_L ratio was calculated, and results were expressed as percentage of control (CHOW WT). ***(E)*** Immunoblot and densitometry of mitochondrial BAD protein. ***(F)*** Measurement of apoptosis of hepatocytes isolated from all experimental groups by flow cytometry (percentage of hypodiploid cells). Data are expressed as mean ± s.e.m (n=4-5 per group). *p<0.05 *vs* CHOW WT. # p<0.05 *vs* HFD WT. †p<0.05 *vs* CHOW KO.

Figure 5. ***Levels of pro-inflammatory cytokines in plasma, liver and adipose tissues.***

(A) Plasmatic levels of IL-6, IL-1β and TNF-α assessed by Luminex analysis. Values are represented as fold increase relative to CHOW WT. ***(B)*** mRNA levels of pro-inflammatory markers measured in liver and ***(C)*** in eWAT by real-time quantitative PCR and normalized to *Gapdh* mRNA expression. Immunoblot analysis of IL-1β Receptor ***(D)*** and TLR4 ***(E)*** expression in hepatic plasma membrane from all experimental groups. Values are expressed as percentage of control (CHOW WT). Data are expressed as mean ± s.e.m (n=4-5 per group). *p<0.05 *vs* CHOW WT. # p<0.05 *vs* HFD WT. †p<0.05 *vs* CHOW KO.

Figure 6. ***Apoptosis and hepatic insulin resistance in HFD-KO mice are IL-1β-dependent.***

Isolated hepatocytes from WT and TNFR1 KO were incubated in DMEM/F12 medium with supplements. Cells were serum starved for 2 h and further stimulated with IL-1β (10ng/ml). After 24 hours cells were stimulated 0, 10 or 50 nM insulin for ***(A)*** p-AKT/AKT expression ratio determination. Values represent fold change to WT (insulin 50 nM without IL-1β). ***(B)*** Immunoblot and densitometric analysis of IRS1 protein level. Values represent percentage of WT without IL-1β. ***(C)*** Caspase-3 activity was evaluated

by a fluorometric assay in hepatocytes treated with or without IL-1β (50 ng/ml). Bar graphs represent Relative Fluorescence Units (RFU). *p<0.05; # p<0.05.

Figure 7. ***TNFR1 signaling disruption increase pro-fibrogenic markers in mice liver under HFD.***

(A) Representative images of Masson's trichromic (MTC) and Sirius Red stained liver paraffin-embedded sections from HFD WT and HFD KO mice. ***(B)*** Quantification of fibrosis score. ***(C)*** Quantification of collagen content. Expressed as percentage area measured in Sirius Red stained slices. Data are expressed as mean ± s.e.m (n=4-5 per group). #p<0.05 *vs* HFD WT.

DISRUPTION OF TUMOR NECROSIS FACTOR ALPHA RECEPTOR 1 SIGNALING ACCELERATES NAFLD PROGRESSION IN MICE UPON A HIGH FAT DIET

Flavia Lambertucci[1], Ainelén Arboatti[1], Guillermina Sedlmeier[1], Omar Motiño[2], María de Luján Alvarez[1], María Paula Ceballos[1], Silvina R Villar[3], Eduardo Roggero[3], Juan A. Monti[1], Gerardo Pisani[4], Ariel D.Quiroga[1], Paloma Martín-Sanz[2,5], Cristina Ester Carnovale[1], Daniel Eleazar Francés[1*] and María Teresa Ronco[1*].

SUPPLEMENTARY RESEARCH DESIGN AND METHODS DATA

Chemicals

Antibodies were from Santa Cruz Biotechnology (Santa Cruz, CA, USA), Sigma Aldrich (St. Louis, MO, USA), Cell Signaling (Boston, MA, USA) and Cayman Chemical (Ann Arbor, MI, USA). Reagents were from Roche Diagnostics (Mannheim, Germany) or Sigma Chemical Co. Human Regular Insulin (Actrapid) was from Novo Nordisk Pharma S.A (Madrid, Spain). Reagents for electrophoresis were obtained from Bio-Rad (Hercules, CA, USA). Tissue culture dishes were from Falcon (Becton Dickinson Labware, Franklin Lakes, NJ, USA). Tissue culture media were from Gibco (InvitrogenTM, Grand Island, NY, USA).

Intraperitoneal Glucose Tolerance Test

Glucose tolerance test (GTT) was performed at the end of the experimental period and after 12 h fasting. After collection of an unchallenged blood sample (time 0), a solution of 20% glucose (2.0 g/kg body mass) was administered into the peritoneal cavity. Blood samples were collected from the tail after 15, 30, 60, 90, and 120 min for determination of glucose concentrations. Glucose levels were measured with an Accu-Check Glucometer

(Roche). Results were shown as blood glucose (mg/dl) in function of time, as well as the area under those curves.

Insulin Tolerance Test

Insulin tolerance test (ITT) was performed after 4h fasting at the end of the experimental period. Insulin (0.5 units/kg body mass) was administered by intraperitoneal injection, and blood samples were collected from the tail vein after 0, 15, 30, 60, 90 min for glucose determination. Results were shown, as blood glucose (mg/dl) in function of time. Glucose levels were measured with an Accu-Check Glucometer (Roche). The constant for glucose disappearance rate during the test (Kitt) was calculated using the formula $(0.693*100)/t_{1/2}$. The glucose $t_{1/2}$ was calculated from the slope of the least-square analysis of the plasma glucose concentrations during the linear decay phase. The HOMA-IR (homeostasis model of assessment of insulin resistance), an index of whole body insulin resistance at basal state, was calculated by HOMA-IR=(FPIxFPG)/22.5; where FPI is fasting plasma insulin concentration (mU/l) and FPG is fasting plasma glucose (mmol/l) [1].

Insulin and cytokine detection

Plasma insulin levels were determined by ELISA kit (Millipore, Billerica, MA, USA) following manufacturer's instructions. Plasma cytokine levels were assessed by Luminex analysis (Luminex 100IS Multiparametric Analyzer).

Histopathology assessment

Hematoxylin-Eosin (H&E) and Masson's trichrome-stained (MTC) paraffin-embedded liver sections were evaluated by the same expertized liver pathologist blinded to the features of animal groups. The NAFLD activity score (NAS) and the fibrosis stage was

assessed using the NAFLD scoring system for mice models validated by Liang *et al.* [2] and Kleiner *et al.* [3]. Briefly, steatosis was graded as follows: grade 0, <5% of steatotic hepatocytes; grade 1, 5–33%; grade 2, >33–66%; and grade 3, >66%. Lobular inflammation was scored as follows: 0, no foci; 1, <2 foci per 200× field; 2, 2-4 foci per 200× field; and 3, >4 foci per 200× field. In addition, fibrosis staging was defined as 0, none; 1, perisinusoidal or periportal; 2, perisinusoidal and portal/periportal; 3, complete central/central bridging fibrosis; and 4, definite cirrhosis.

Light microscopic analysis of hematoxylin and eosin stained slides was used to count the percent of apoptotic cells. An apoptotic index (AI) was calculated for each sample by counting the number of positively stained hepatocyte nuclei divided by the total number of hepatocytes and expressed as percentage. The number of apoptotic hepatocytes was assessed by systematically scoring at least 6000 hepatocytes per slide at a magnification of 400× [4].

Apoptotic cells were detected with the TUNEL-based *In Situ* Cell Detection Kit (*In situ* cell death fluorescein, Sigma). Sections were deparaffinized, hydrated, and digested with proteinase K (Dako) for 30 min at 37°C and then subjected to the TUNEL reaction according to the manufacturer's instructions; TUNEL-positive cells were visualized using a standard immunofluorescence microscope (CTR600, Leica) [5].

Quantitative analysis of collagen in Sirius Red-stained liver sections was performed using imaging analysis software (ImageJ software (http://imagej.nih.gov)). Briefly, paraffin sections of 20 μm thickness were stained in 0.1% Sirius red in saturated picric acid. The red-stained area (μm^2) was measured in five consecutive fields (40×). Fibrotic area percentage was calculated relative to the total area examined [6].

RNA isolation, cDNA synthesis, and real-time quantitative polymerase chain reaction

Total liver RNA was isolated by the TRIzol method (Life Technologies, Inc., Gaithersburg, MD, USA) according to manufacturer's instructions. One microgram of total liver RNA was treated with DNase I (Thermo Fisher Scientific) and cDNA was synthesized using an oligodT primer and MultiScribe™ Reverse Transcriptase (Life Technologies, Inc., Gaithersburg, MD, USA). Polymerase chain reaction (PCR) assay was performed using the StepOne™ Real-Time PCR System (Applied Biosystems, U.S.A.) with SYBR® Green PCR Master Mix (Life Technologies, Inc., Gaithersburg, MD, USA) according to manufacturer's instructions. The PCR conditions were: 10 min at 95 °C, followed by 40 cycles of a two-step PCR denaturation at 95 °C for 15 s and annealing/extension at 60 °C for 60 s. For each sample we analyzed gapdh (*in vivo* studies) expression to normalize target gene expression. Primers were designed using Primer3 software [7] and were then manufactured by Invitrogen. The list of genes with their primer sequences and PCR product size are given in Supplementary table 2. Relative changes in gene expression were determined by using the $2^{-\Delta\Delta Ct}$ method [8].The replicates were then averaged, and fold induction was determined in a ΔΔCt based fold-change calculations.

Western blot analysis

Fractions enriched in plasma membranes were obtained by centrifugation at 56,000 rpm for 60 min on a discontinuous 1.3 M sucrose gradient, as described [9]. Mitochondria-enriched fractions were obtained by centrifugation at 3000g at 4° C for 15min. Liver tissue and hepatocytes lysates were prepared by homogenization in 3 volumes of lysis RIPA buffer containing PBS, 1% Triton X-100, 0.5% sodium deoxycholate, 0.1% SDS, 1mM phenylmethylsulfonyl fluoride, 10μg/ml leupeptin, and 1μg/ml aprotinin; and centrifugation

at 15,000 rpm for 30 min. [10]. Proteins were quantified according to Lowry technique For Western blot analysis, equal amounts of protein (20-30 µg) were separated by 10-15% SDS-polyacrylamide electrophoresis gel (SDS-PAGE). The relative amounts of each protein were determined with the following polyclonal or monoclonal antibodies (Supplementary table 3). After incubation with the corresponding anti-rabbit or anti-mouse horseradish peroxidase conjugated secondary antibody, blots were developed by the ECL protocol (Amersham). Target protein band densities were normalized with the corresponding antibody. Immunoreactive bands were quantified by densitometry using the Image J software (imagej.nih.gov).

Caspase-3 activity assay

The activity of caspase-3 was determined according to the manufacturer's instructions using an EnzChekTM caspase-3 assay kit (Molecular Probes,USA), as we previously reported [11]. Briefly, tissues were homogenized in lysis buffer. After differential centrifugation, the cytosolic fraction from each sample was mixed with Z-Asp-Glu-Val-Asp-7-Amino-4-Methyl-Coumarin (Z-Asp-Glu-Val-Asp-AMC) substrate solution. A standard curve of AMC ranging from 0 to100mM was run with each set of samples. A control sample without enzyme was used in each assay to assess the background fluorescence of the substrate. As an additional control, 1µl of 1 mM Ac-Asp-Glu-Val- Asp-CHO (aldehyde), the caspase-3 inhibitor stock solution, was added. Fluorescence was measured at an excitation wavelength of 360nm and an emission wavelength of 465nm in a DTX880 multimode detector (Beckman Coulter).

In vitro studies

Isolation and culture of mouse hepatocytes

Hepatocytes were isolated from non-fasting male WT and TNFR1 KO mice by perfusion with collagenase [12]. Cells were plated in 6-cm dishes and cultured in DMEM/F12 medium supplemented with 100 U/ml penicillin, 100 μg/ml streptomycin and 10% FBS for 16 h. Cells were serum starved for 2 h and further stimulated with IL1β (10 ng/ml or 50ng/ml). For insulin signaling studies, after 24 hours cells were stimulated with 0, 10 or 50 nM insulin for 7 min.

Isolation of hepatic non-parenchymal cells (NPCs) for flow cytometry analysis

Hepatic non-parenchymal cells were isolated as described previously [13] with some modifications. Briefly, liver tissue was perfused with collagenase, mashed through a cell strainer (100 μm), centrifuged at 500 g for 5 min at RT and the cell pellet resuspended in 36% Percoll-HBSS solution. After centrifugation at 800 g for 20 min without brake, erythrocyte lysis was performed for 10 min at RT in 139 mM NH_4Cl, 19 mM Tris–HCl pH 7.2 solution, washed the pellet twice, and suspended in 100 μl of PBS.

Flow cytometry

NPC cells ($0.3–0.5 \times 10^6$ cells/test) were incubated for 20 min at RT in the dark with the following antibodies (5 μg/ml): CD11b-Mac1- PECy7 (rat IgG2bk, anti-mouse eBioscience, San Diego CA, USA), CD45-FITC (rat IgG, Beckman), F4/80-PE (ratIgG2ak, eBioscience), CCR2-APC (ratIgG2B, R&DSystems, Minneapolis, MN, USA) or their corresponding isotype controls. Flow cytometry analysis was performed using Cell Sorter BD FACSAria II, BD Biosciences.

Quantification of apoptotic cells by flow cytometry

Isolated hepatocytes were centrifuged, washed with PBS, and fixed with cold ethanol. The cells were then washed, resuspended in PBS, and incubated with RNase A (25 mg/10^6 cells) for 30 min at 37ºC, as previously described [14]. After addition of 0.05% propidium iodide, the cells were analyzed by flow cytometry (Cell Sorter BD FACSAria II, BD Biosciences). All data were analyzed with WinMDi (http://facs.scripps.edu/software.html) and Cylchred Software.

REFERENCES

[1] Francés DE, Motiño O, Agrá N, González-Rodríguez A, Fernández-Álvarez A, Cucarella C, et al. Hepatic cyclooxygenase-2 expression protects against diet-induced steatosis, obesity and insulin resistance. Diabetes 2015;64:1522–31. doi:10.2337/db14-0979.

[2] Liang W, Menke AL, Driessen A, Koek GH, Lindeman JH, Stoop R, et al. Establishment of a general NAFLD scoring system for rodent models and comparison to human liver pathology. PLoS One 2014;9:e115922. doi:10.1371/journal.pone.0115922.

[3] Kleiner DE, Brunt EM, Van Natta M, Behling C, Contos MJ, Cummings OW, et al. Design and validation of a histological scoring system for nonalcoholic fatty liver disease. Hepatology 2005;41:1313–21. doi:10.1002/hep.20701.

[4] Ronco MT, Francés DE, Ingaramo PI, Quiroga AD, Alvarez ML, Pisani GB, et al. Tumor necrosis factor alpha induced by Trypanosoma cruzi infection mediates inflammation and cell death in the liver of infected mice. Cytokine 2010;49:64–72. doi:10.1016/j.cyto.2009.09.012.

[5] Rico M, Baglioni M, Bondarenko M, Laluce NC, Rozados V, André N, et al. Metformin and propranolol combination prevents cancer progression and metastasis in different breast cancer models. Oncotarget 2017;8:2874–89. doi:10.18632/oncotarget.13760.

[6] Motiño O, Agra N, Brea Contreras R, Domínguez-Moreno M, García-Monzón C, Vargas-Castrillón J, et al. Cyclooxygenase-2 expression in hepatocytes attenuates non-alcoholic steatohepatitis and liver fibrosis in mice. Biochim Biophys Acta 2016;1862:1710–23. doi:10.1016/j.bbadis.2016.06.009.

[7] Rozen S, Skaletsky H. Primer3 on the WWW for general users and for biologist programmers. Methods Mol Biol 2000;132:365–86.

[8] Lardizábal MN, Nocito AL, Daniele SM, Ornella LA, Palatnik JF, Veggi LM, et al. Reference genes for real-time PCR quantification of microRNAs and messenger RNAs in rat models of hepatotoxicity. PLoS One 2012;7:e36323. doi:10.1371/journal.pone.0036323.

[9] Ronco MT, Manarin R, Francés D, Serra E, Revelli S, Carnovale C. Benznidazole treatment attenuates liver NF-κB activity and MAPK in a cecal ligation and puncture model of sepsis. Mol Immunol 2011;48:867–73. doi:10.1016/j.molimm.2010.12.021.

[10] Lambertucci F, Motiño O, Villar S, Rigalli JP, de Luján Alvarez M, Catania V, et al. Benznidazole, the trypanocidal drug used for Chagas disease, induces hepatic NRF2 activation and attenuates the inflammatory response in a murine model of sepsis. Toxicol Appl Pharmacol 2017;315:12–22. doi:10.1016/j.taap.2016.11.015.

[11] Ingaramo PI, Ronco MT, Francés DEA, Monti JA, Pisani GB, Ceballos MP, et al. Tumor necrosis factor alpha pathways develops liver apoptosis in type 1 diabetes mellitus. Mol Immunol 2011;48:1397–407. doi:10.1016/j.molimm.2011.03.015.

[12] Parody JP, Ceballos MP, Quiroga AD, Frances DE, Carnovale CE, Pisani GB, et al. FoxO3a modulation and promotion of apoptosis by interferon-??2b in rat preneoplastic liver. Liver Int 2013:1566–77. doi:10.1111/liv.12421.

[13] Sanz-Garcia C, Ferrer-Mayorga G, Gonzalez-Rodriguez A, Valverde AM, Martin-Duce A, Velasco-Martin JP, et al. Sterile Inflammation in Acetaminophen-induced Liver Injury Is Mediated by Cot/tpl2. J Biol Chem 2013;288:15342–51. doi:10.1074/jbc.M112.439547.

[14] Pilar Valdecantos M, Prieto-Hontoria PL, Pardo V, Módol T, Santamaría B, Weber

M, et al. Essential role of Nrf2 in the protective effect of lipoic acid against lipoapoptosis in hepatocytes. Free Radic Biol Med 2015;84:263–78. doi:10.1016/j.freeradbiomed.2015.03.019.

Figure 1

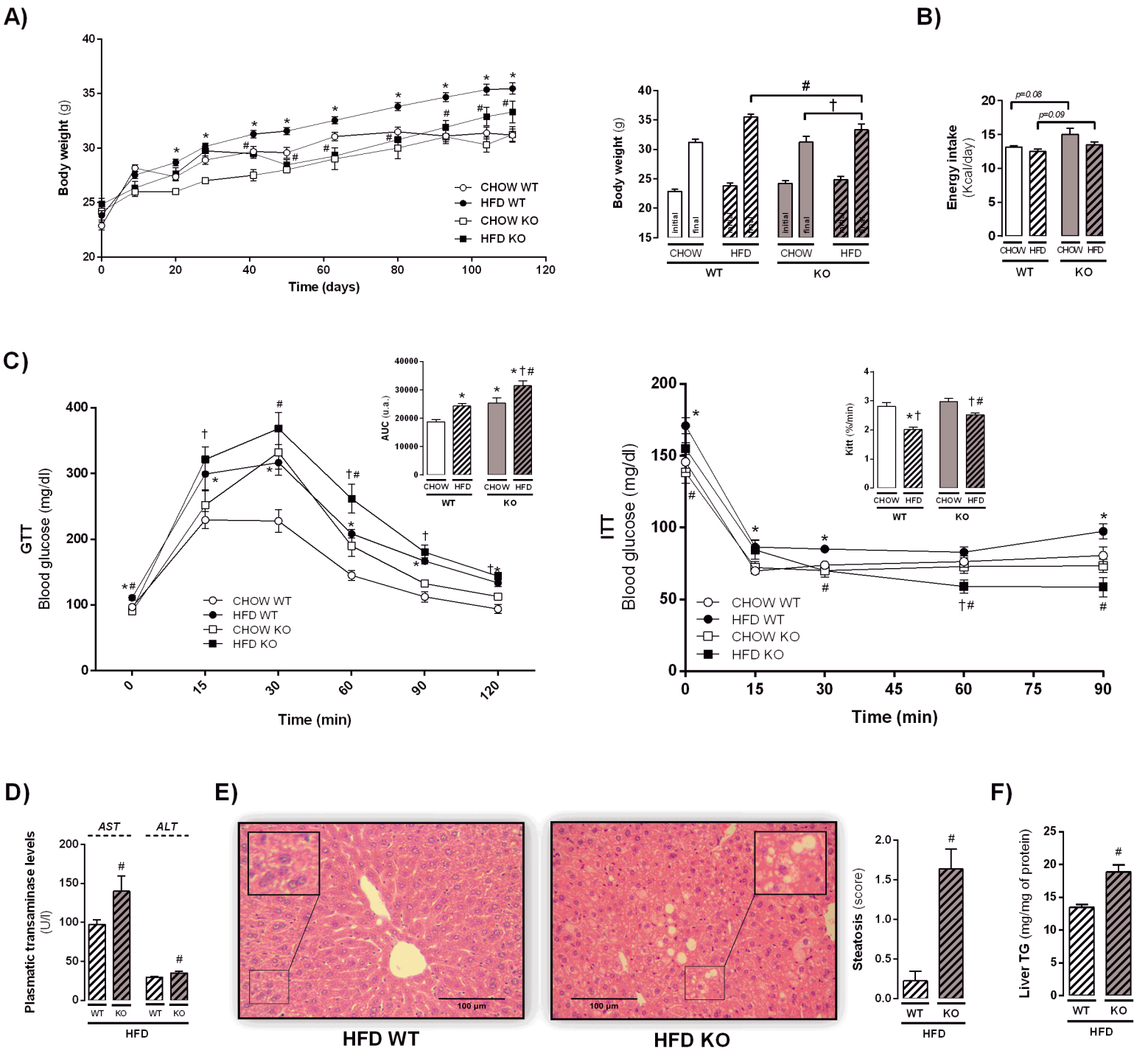
A)
Body weight (g)
Time (days)
CHOW WT
HFD WT
CHOW KO
HFD KO
Body weight (g)
initial
final
CHOW
HFD
WT
KO
B)
Energy intake (Kcal/day)
p=0.08
p=0.09
C)
GTT
Blood glucose (mg/dl)
Time (min)
AUC (u.a.)
ITT
Kitt (%/min)
D)
Plasmatic transaminase levels (U/l)
AST
ALT
E)
100 µm
HFD WT
HFD KO
Steatosis (score)
F)
Liver TG (mg/mg of protein)

Figure 2

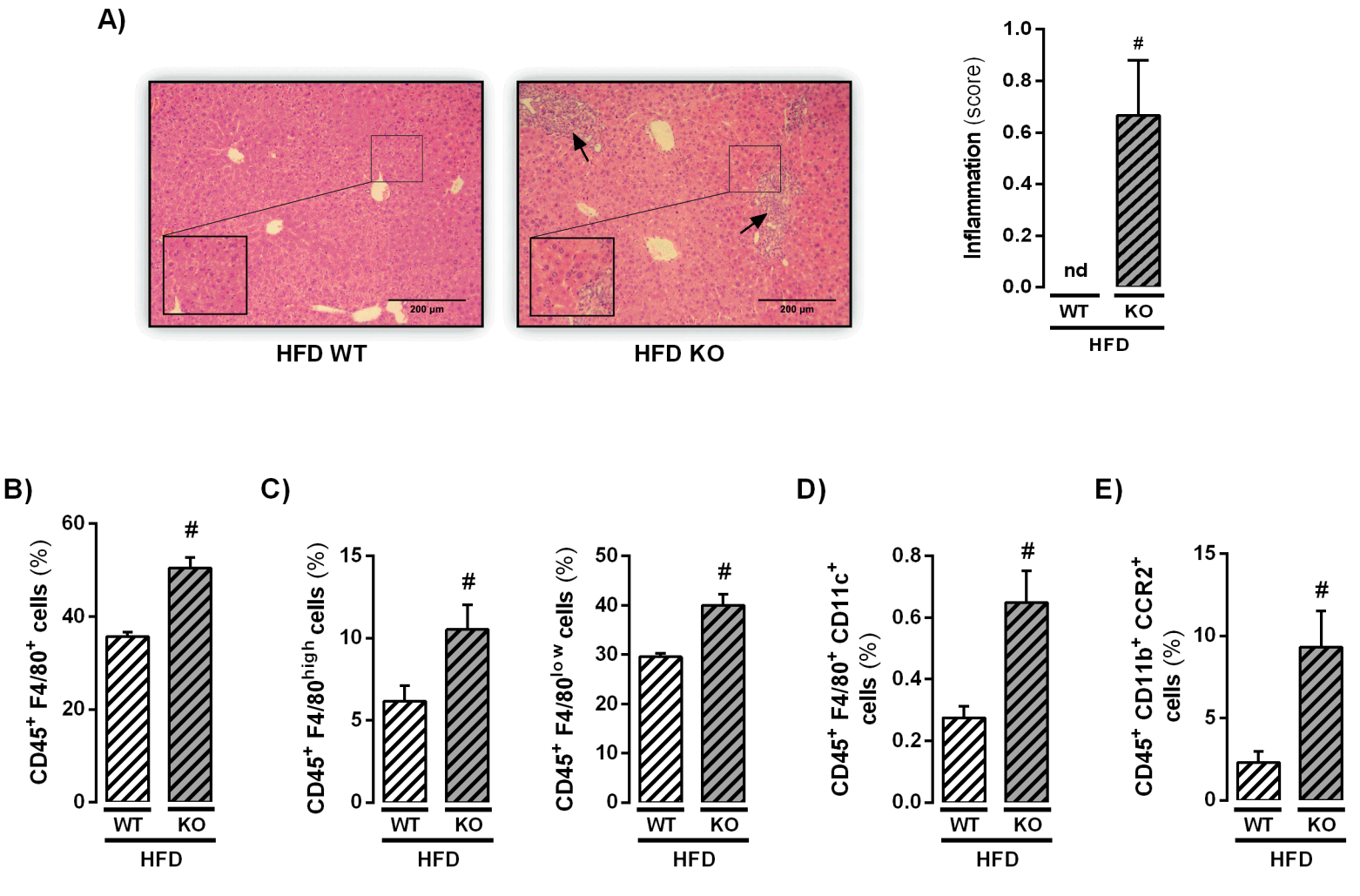
A)
200 µm
200 µm
HFD WT
HFD KO
Inflammation (score)
1.0
0.8
0.6
0.4
0.2
0.0
nd
#
WT
KO
HFD
B)
CD45+ F4/80+ cells (%)
60
40
20
0
#
WT
KO
HFD
C)
CD45+ F4/80high cells (%)
15
10
5
0
#
WT
KO
HFD
CD45+ F4/80low cells (%)
50
40
30
20
10
0
#
WT
KO
HFD
D)
CD45+ F4/80+ CD11c+ cells (%)
0.8
0.6
0.4
0.2
0.0
#
WT
KO
HFD
E)
CD45+ CD11b+ CCR2+ cells (%)
15
10
5
0
#
WT
KO
HFD

Figure 3

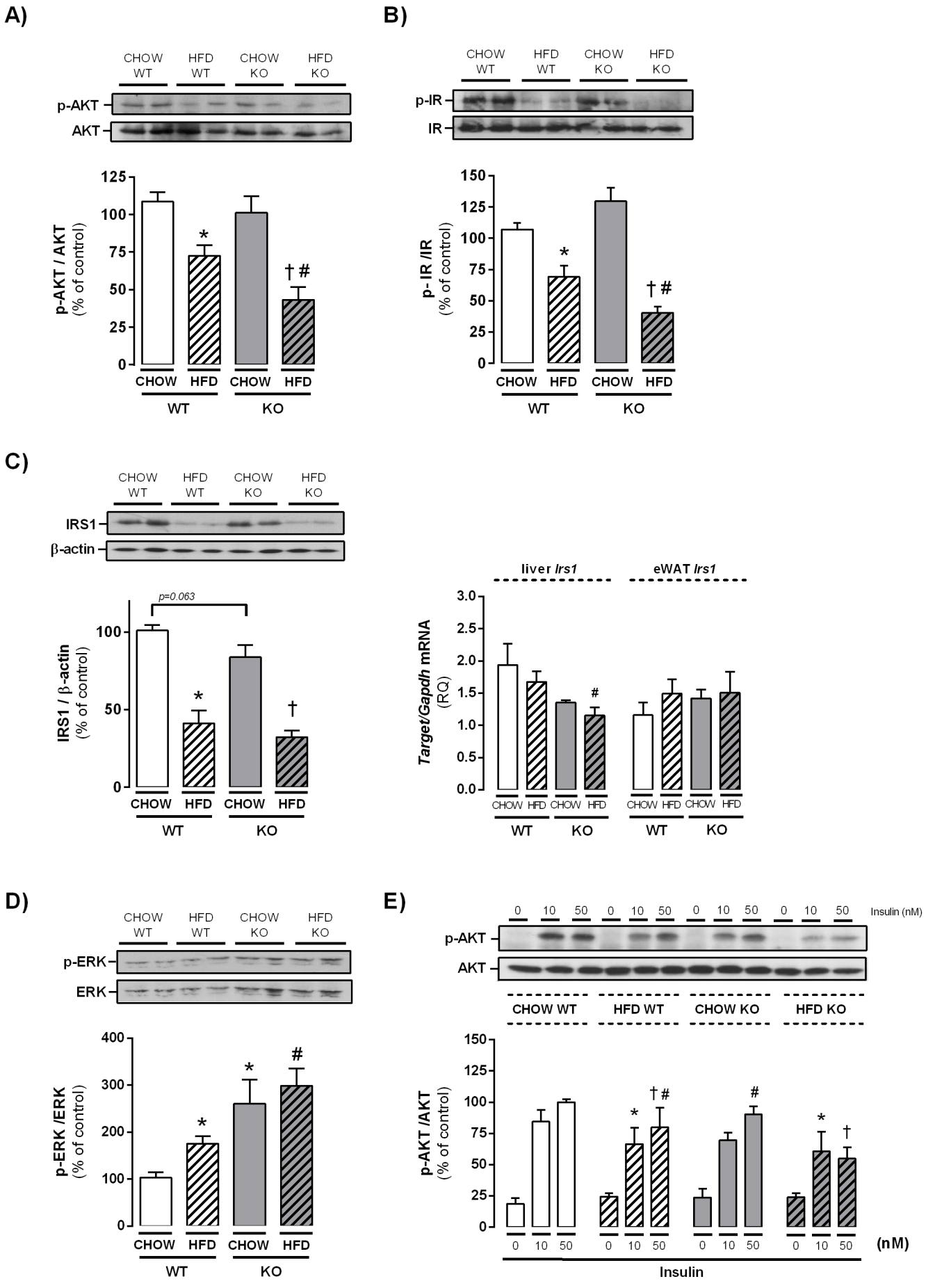
A)
CHOW WT
HFD WT
CHOW KO
HFD KO
p-AKT
AKT
p-AKT / AKT (% of control)
CHOW HFD CHOW HFD
WT KO
B)
p-IR
IR
p- IR /IR (% of control)
C)
IRS1
β-actin
p=0.063
IRS1 / β-actin (% of control)
liver lrs1
eWAT lrs1
Target/Gapdh mRNA (RQ)
D)
p-ERK
ERK
p-ERK /ERK (% of control)
E)
Insulin (nM)
p-AKT /AKT (% of control)
(nM)
Insulin

Figure 4

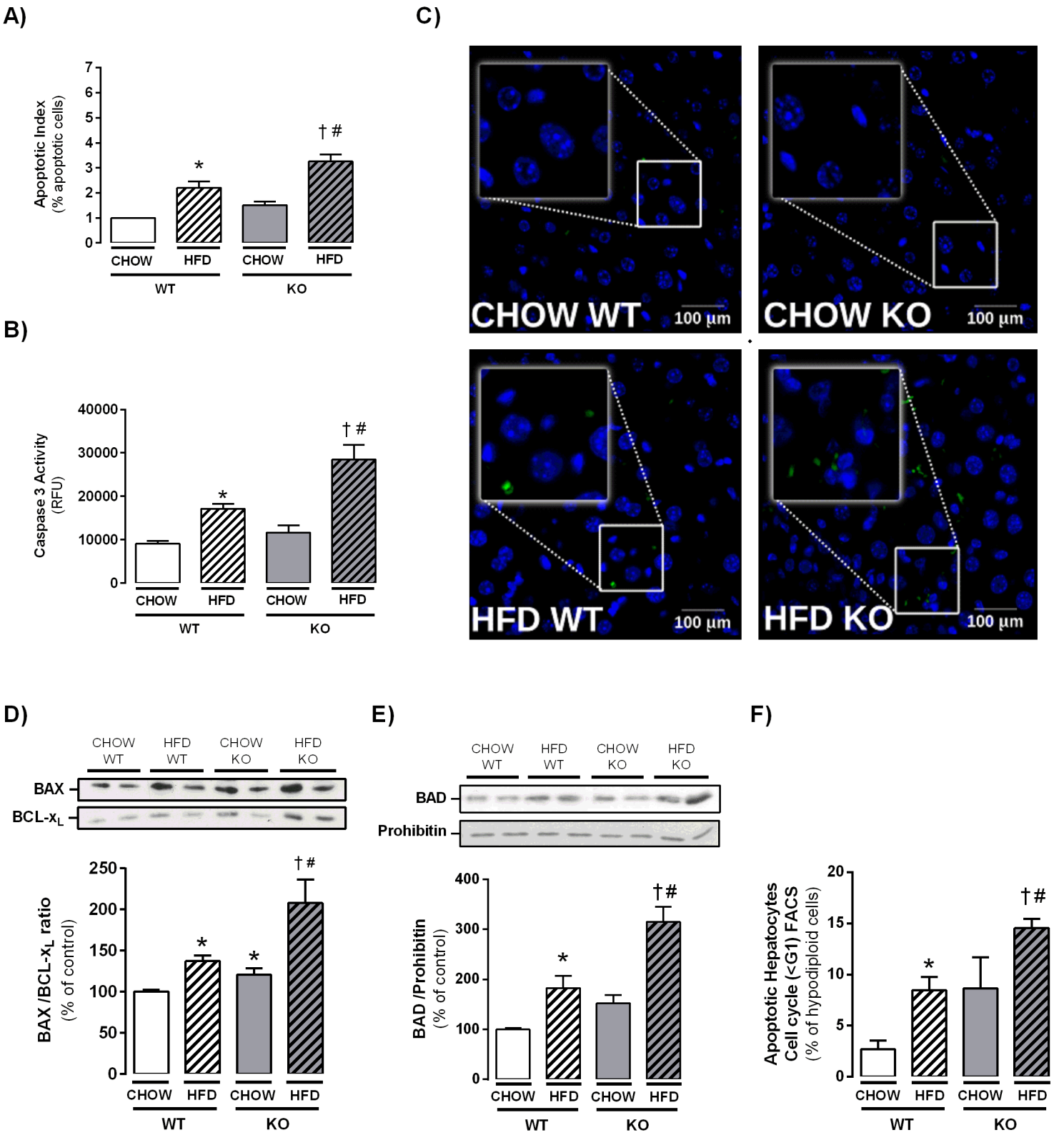
A)
Apoptotic Index
(% apoptotic cells)
CHOW
HFD
CHOW
HFD
WT
KO
B)
Caspase 3 Activity
(RFU)
CHOW
HFD
CHOW
HFD
WT
KO
C)
CHOW WT
100 µm
CHOW KO
100 µm
HFD WT
100 µm
HFD KO
100 µm
D)
CHOW WT
HFD WT
CHOW KO
HFD KO
BAX
BCL-xL
BAX /BCL-xL ratio
(% of control)
CHOW
HFD
CHOW
HFD
WT
KO
E)
CHOW WT
HFD WT
CHOW KO
HFD KO
BAD
Prohibitin
BAD /Prohibitin
(% of control)
CHOW
HFD
CHOW
HFD
WT
KO
F)
Apoptotic Hepatocytes
Cell cycle (<G1) FACS
(% of hypodiploid cells)
CHOW
HFD
CHOW
HFD
WT
KO

Figure 5

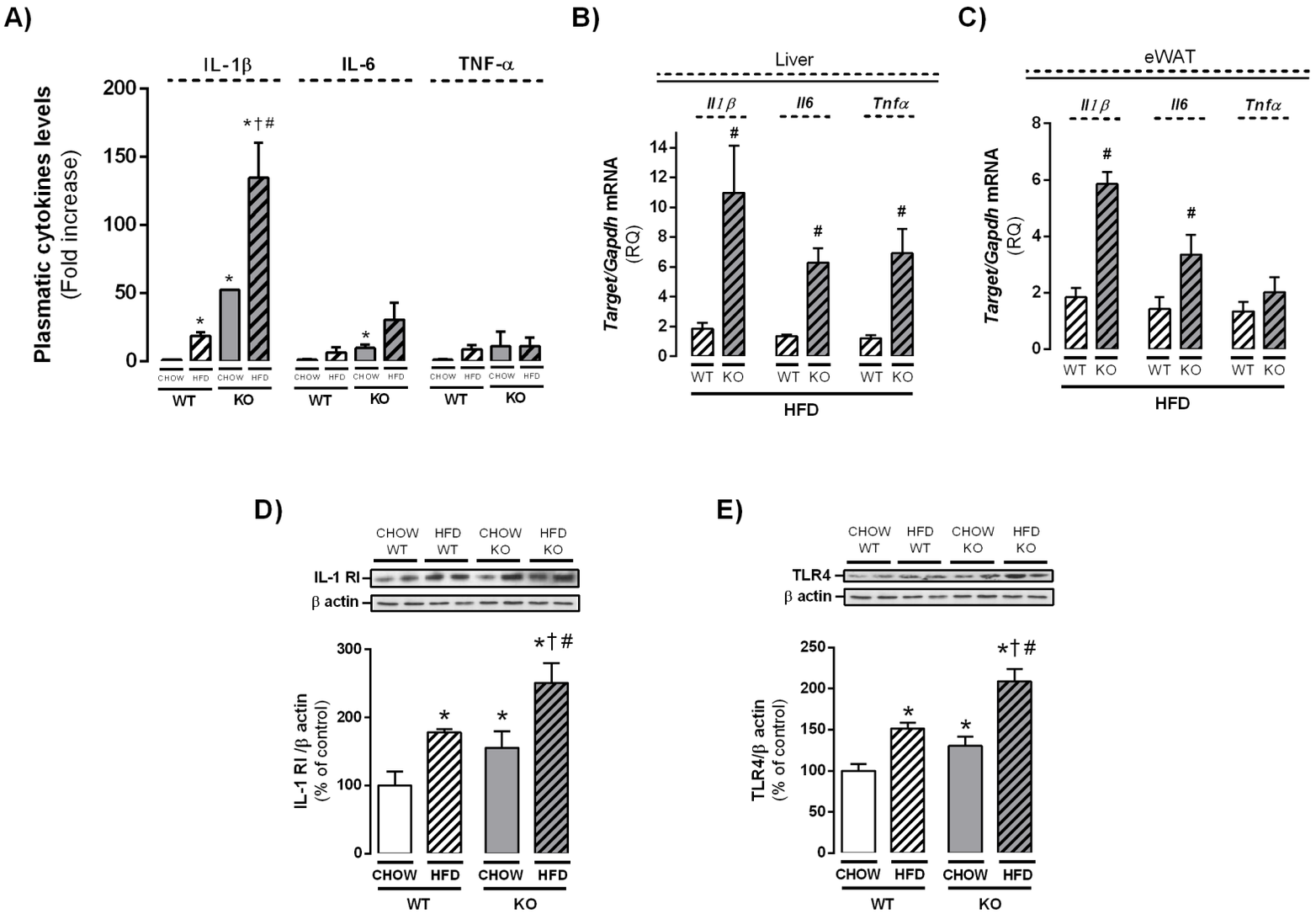
A)
IL-1β
IL-6
TNF-α
Plasmatic cytokines levels
(Fold increase)
200
150
100
50
0
*†#
*
*
*
CHOW HFD CHOW HFD
WT
KO
WT
KO
WT
KO
B)
Liver
Il1β
Il6
Tnfα
Target/Gapdh mRNA
(RQ)
14
12
10
8
6
4
2
0
#
#
#
WT KO WT KO WT KO
HFD
C)
eWAT
Il1β
Il6
Tnfα
Target/Gapdh mRNA
(RQ)
8
6
4
2
0
#
#
WT KO WT KO WT KO
HFD
D)
CHOW WT
HFD WT
CHOW KO
HFD KO
IL-1 RI
β actin
IL-1 RI /β actin
(% of control)
300
200
100
0
*†#
*
*
CHOW HFD CHOW HFD
WT
KO
E)
CHOW WT
HFD WT
CHOW KO
HFD KO
TLR4
β actin
TLR4/β actin
(% of control)
250
200
150
100
50
0
*†#
*
*
CHOW HFD CHOW HFD
WT
KO

Figure 6

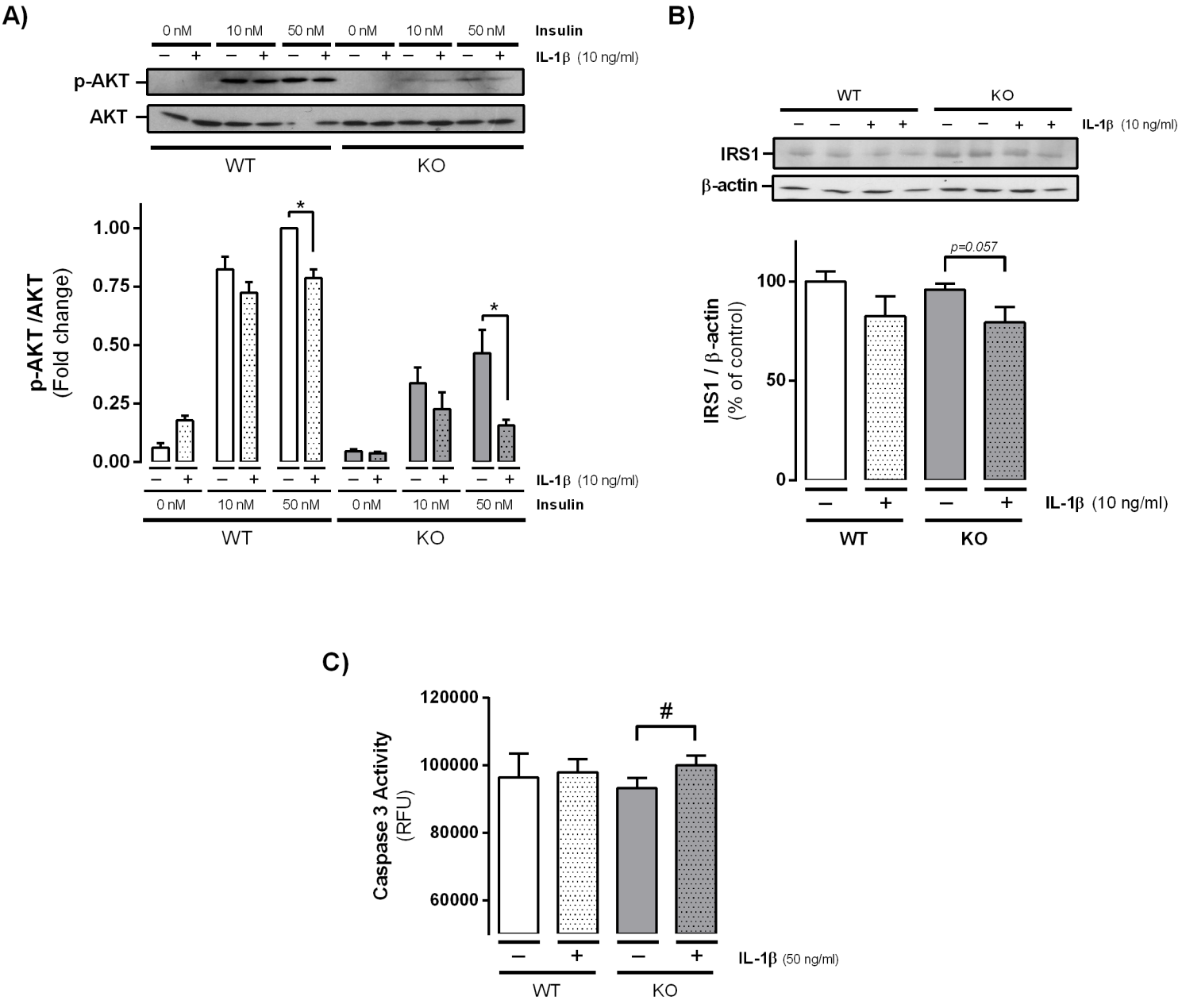
A)
0 nM
10 nM
50 nM
0 nM
10 nM
50 nM
Insulin
IL-1β (10 ng/ml)
p-AKT
AKT
WT
KO
p-AKT /AKT
(Fold change)
1.00
0.75
0.50
0.25
0.00
*
*
IL-1β (10 ng/ml)
Insulin
B)
WT
KO
IL-1β (10 ng/ml)
IRS1
β-actin
p=0.057
IRS1 / β-actin
(% of control)
100
50
0
IL-1β (10 ng/ml)
C)
Caspase 3 Activity
(RFU)
120000
100000
80000
60000
#
IL-1β (50 ng/ml)

Figure 7

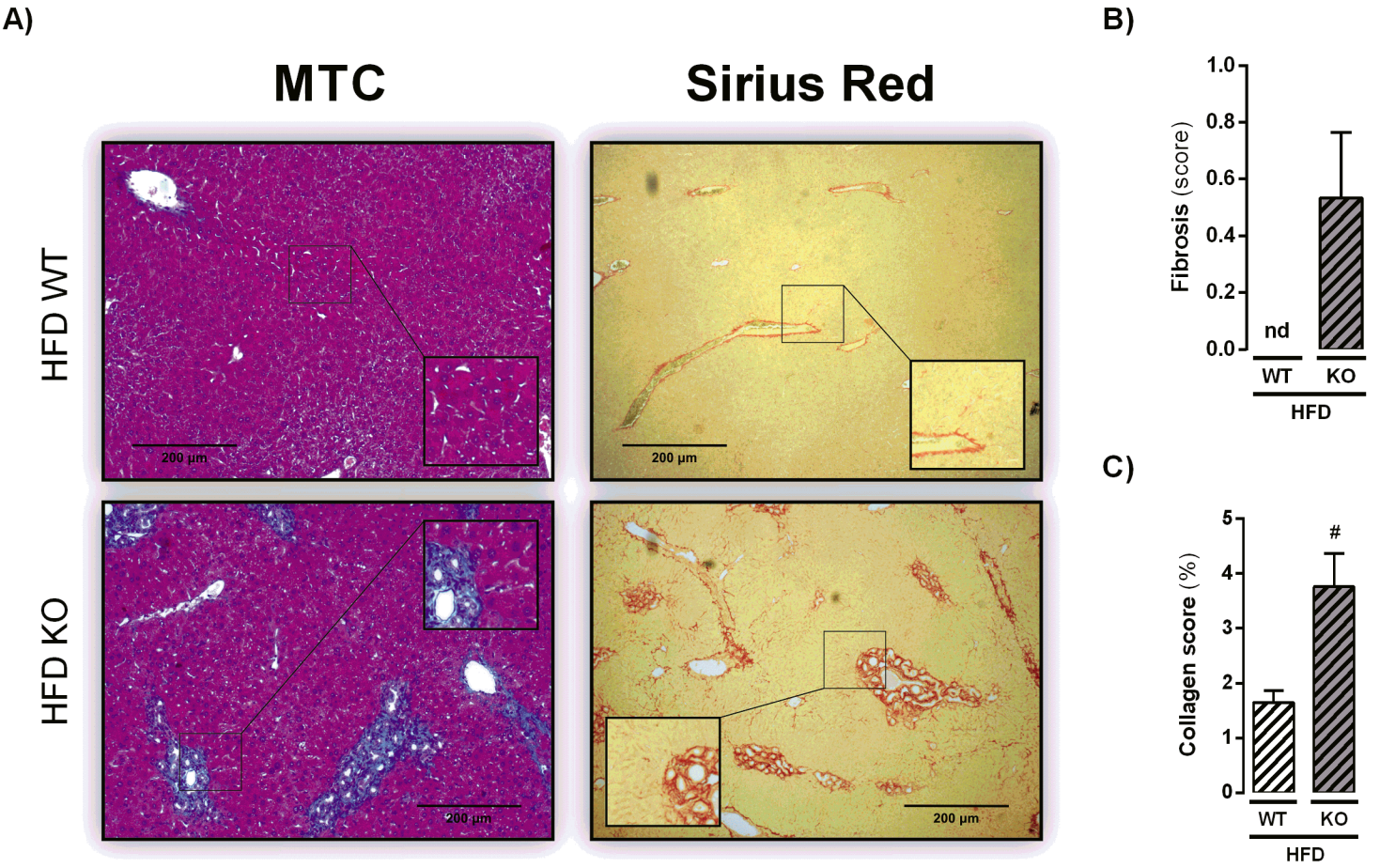
A)
MTC
Sirius Red
HFD WT
HFD KO
200 µm
200 µm
200 µm
200 µm
B)
Fibrosis (score)
1.0
0.8
0.6
0.4
0.2
0.0
nd
WT
KO
HFD
C)
Collagen score (%)
5
4
3
2
1
0
#
WT
KO
HFD